Linnæus University
Sweden

Thermo-Mechanical Fatigue Assessment of Marine Boiler

Using linear Finite Element Analyses

Author: Samuel Alagbada
Supervisor: Per Lindström
Examiner: Lars Håkansson
Term: VT20
Subject: Mechanical Engineering
Level: Advanced
Course code: 4MT31E

Abstract

This thesis is on fatigue crack growth assessments of a thermomechanical loaded Marine Boiler- Sunrod CPDB12. The installation position of the marine boiler in the ship in relation to its fatigue life under mode 1 loading is investigated. Thermomechanical loading embodies pressures, temperatures, RAO, subjected to the rigid body dynamic of ship in the marine environment.

Linear elastic fracture mechanics (LEFM) method was used is predicting the growth rates of the welding flaws at the joint based on stress range of the Paris law relationship. FEA Numerical simulation delivered better crack growth rate assessments and life predictions of the smallest detectable flaws in the boiler.

The identified smallest detestable flaws at the welding joint diminishing the designed safe life of the boiler significantly. Also, installation position within the ship do affect the fatigue life of the boiler.

Key words

Marine Boiler, FEA, Thermo-mechanical Loading, LEFM, Paris law, Flaws, RAO.

Acknowledgments

My profound gratitude goes to all who has being part of this journey from inception.

The author extends his gratitude toward Mr. Sohail Anwar for a great initial cooperation of this study where the interventions of the destiny eventually separated us.

The great job in the pursuit of excellences by the mechanical engineering department of Linnaeus University is appreciated.

Finally, my sincere appreciation of all the family members for providing me with their unalloyed support always.

Table of contents

Appendices

Scalars

A	Area of the boiler [m²]
BM	Metacentric radius
C	Crack growth parameter
CB	Block Coefficient
CM	Metacentric Centre
COB	Centre of Buoyancy
COG	Centre of Gravity
$\mathbf{D}$	Accumulated fatigue damage
$\boldsymbol{E}$	Material modulus of elasticity (Young´s modulus) [$\mathrm{N/m^2}$]
$\boldsymbol{E_1}$	Elastic modulus temperature dependence [$\mathrm{N/m^2}$]
GM	The vessel's metacentric height
KG	Height of centre of gravity above the keel
KM	Height of metacentre above keel
$\boldsymbol{L}$	Length of the vessel [m]
P	Pressure [Pa]
R	Height Parameter [m]
$\boldsymbol{R}$	Stress Ratio
RAO	Response Amplitude Operators,
T	Absolute temperature [K]
TLC	Draft at midship in considered loading conditions
$\boldsymbol{\Delta K_{th}}$	Threshold stress intensity factor range
$\boldsymbol{a_i}$	Initial crack size [mm]
$\boldsymbol{a_f}$	Final crack size [mm]
$\boldsymbol{a_o}$	Acceleration parameter of the Ship
$\boldsymbol{a_{heave}}$	Translational acceleration of the ship y- direction [m/s^2]
$\boldsymbol{a_{pitch}}$	Rotational Movement in Z direction [m/s^2]
$\boldsymbol{a_{roll}}$	Rotational Movement in X direction [m/s^2]
$\boldsymbol{a_{surge}}$	Translational acceleration of the ship x- direction [m/s^2]
$\boldsymbol{a_{Sway}}$	Translational acceleration of the ship z- direction [m/s^2]
$\boldsymbol{a_{yaw}}$	Rotational Movement in Y direction [Rad/s^2]
g	Gravitational acceleration [m/s²]
k	Number of stress blocks
$\boldsymbol{k_r}$	Radius of gyration of roll
$\boldsymbol{l_f}$	The design lifetime
$\boldsymbol{n_i}$	Number of applied stress cycles at the i-th stress range
$\boldsymbol{N_i}$	Number of cycles to failure at constant stress range
m	Exponent of the Paris-Erdogan power law
x	Perpendicular distance from the boiler [m]
W	Width of the vessel [m]
$\boldsymbol{\sigma_a}$	Alternating stress [$\mathrm{N/m^2}$]
$\boldsymbol{\sigma_m}$	Mean stress [$\mathrm{N/m^2}$]
$\boldsymbol{\sigma_{max}}$	Stress maximum in stress history [$\mathrm{N/m^2}$]
$\boldsymbol{\sigma_{min}}$	Stress minimum in stress history [$\mathrm{N/m^2}$]
$\boldsymbol{\Delta\sigma}$	Stress range

1 Introduction.

1.1 Background and problem description

Boiler technology started as far back as 200 B.C with a Greek engineer named Hero who designed a simple rotary steam engine machine ‘Aelopile’ that used steam as its power source for pumping water from the mines. The Aelopile is the first device known to transform steam into rotary motion as result of personal curiosity of in the field of invention exploration using hollow sphere mounted on a cauldron so that it could turn on a pair of hollow tubes that would provide steam to the sphere of a cauldron. The steam generated escaped from the sphere from one or more bent tubes projecting from its equator, causing the sphere to revolve [1] as illustrated in *Figure 1*

Figure 1: Artistic illustration of the Aelopile [2] Public Domain

George Babcock and Steven Wilcox were two of the founding fathers of the steam-generating boiler. In 1867, They were the first to patent (Babcock & Wilcox Company in New York City) their boiler design, which used tubes inside a firebrick-walled structure to generate steam, the solid firebrick walls that formed the enclosure for the unit were necessary because they helped the combustion process by reradiating heat back into the furnace area. Although their first boilers were quite small, used lump coal, fired by hand, and operated at a very low rate of heat input.[1], [3] [4].

In the early days of the steam boiler manufacturing the pressure retaining shell plates were joined by overlapping rivet joint seam, a joining technology notorious known for its tendency to start leaking after just a few thermo-mechanical fatigue load cycles. This situation motivated the Swedish Marine Engineer Oscar Kjellberg to invent the Metal Arc Welding process (SMAW), so called stick welding in the early 1900’s.The industrial revolution of the nineteenth century produced Scottish boilers in meeting the higher steam production and pressures required for powering steam turbines in marine warship [5].

Marine Boilers are pressurized heat exchange system that produces steam for various operational purposes in a ship or offshore rig and they are divided into three categories [5]:

I. Main boilers, supplying steam for the propulsion of a ship.

II. Auxiliary boiler supplies steam for heating of accommodations, fuel and cargo and to drive auxiliary equipment like cargo pump turbines.

III. Exhaust gas boilers are installed on almost all ships and rigs to increase the overall efficiency by utilizing the waste heat in the exhaust gases.

Also, marine boilers could be further classified according to method of manufacture/ construction as shell, horizontal, vertical and water tube types [5].

Marine boilers' accident reports during the industrial revolution of the 19th century were unfortunate and common part of history, thereby, initiated a series of technological advancement, which shaped the world of Boiler for reliability and safety as core pursuit of all (mechanical Engineers, Researchers, designer and legislation)[6][7].Frequent occurrence of such accidents were fatigue related which has been an incentive for investigating its mechanism of failure for more than 160 years in order to have a reliable lifetime prediction methodology that would have a major societal impact in terms of both economics and safety [8]-[10]. According to [10] the USA national costs associated with material fractures for a single year (1978) was $119 billion or 4% of the USA Gross National Product. Fatigue accounted for 80% of the failures investigated in fire tube boilers and 28% in water tube boilers [9],which has as a major issue that spans several engineering disciplines and costs hundreds of billions of dollars thereof[10]. Also in Year 2017,ASME diary still had some recent thermo-mechanical fatigue failures such as Marine auxiliary Boiler explosion accident of a container ship m/s Manhattan bridge at the port of Flex atone, United Kingdom 2017 leaving the duty oiler died and the injuries of various degree of the engineer onboard thereby necessitated a continuous investigation, analyses of all possible root causes and remodelling of marine boilers in reducing thermo-mechanical fatigue failures[11].

Significant progress in the field of engineering were achieved globally in ensuring zero fatigue related failure of a marine boiler with Periodical Inauguration of Dedicated American Society Of Mechanical Engineering (ASME) research conference in conjunction with designers, engineers and scientist. The proceedings of the conferences, Journals, books, and standards reflecting the knowledge and experimental capabilities from mid-seventies till today [7].

Records had it that the number of marine steam boiler and marine steam pressure vessels accidents have decreased, but it is still a life threatening and operational obstacle for the marine and/or shipping industry with respect to recent accidents log.[6][8]

From the literature survey [1]-[17] the present authors have understood that the most common causes of boiler failures is fatigue. Fatigue is a progressive transient decrease of material strength as a result of the application of cyclic mechanical load.

The fast heating and cooling cycles cause thermally induced strains and stresses, which often operate in combination with the mechanical load cycles of the steam pressure variations. The resulting thermo-mechanical fatigue cycle leads to material degradation mechanisms and failure modes typical of service [13][14].

Nevertheless, marine boiler are not only prone to fatigue failure due to its thermo-mechanical load cases, in addition to that they are also affected by the accelerations of the ocean waves, which is approximated by so called sea keeping analysis[13]. Furthermore, one has over time understood that marine boiler weld joints, like all other weld joints, are sensitive to fatigue failure due to the interaction of the Weld Residual Affected Zone (WRAZ) and the Heat Affected Zone (HAZ), both created by the manufacturing arc welding process [15].

Also, the present author have understood that other common root causes for boiler failures are fatigue related to corrosion and erosions phenomena of the material such as general surface corrosion, pitting corrosion, flow accelerated corrosion, cavitation, fluid erosion Corrosion and stress-corrosion cracking as well as overheating due to thermal transfer barriers of deposits and gas waterside fouling e.g. bad seamen ship, thereby resulting in increased material stresses[18].

By statutory requirements marine boilers must by be designed, engineered and manufactured in accordance with the highest Rules of a Classification Society that is recognized by the actual ship's Maritime Administration [16].It implies that all aforementioned marine boiler explosions have occurred on boilers of the highest class and/or approved by each single ship's Maritime Administration.

Recently two marine engineers [18] presented a fatigue analysis report of a marine steam boiler of the design type Sunrod CPDB12, in *Figure 3*. They examined the boiler's failure case as lack of fusion in the longitudinal direction of the boiler's shell plate weld joint, where conventional Non Destructive Test (NDT) methods were used on the flaw dimension for the smallest detectable crack size according to [17]. They recommended further research for more exact approximation of the boiler's fatigue lifetime by the use of Finite Element Method (FEM) so called Finite Element Analysis (FEA).

It implies that the author have identified all controversies where ship classification societies claims [5] that the explosion are more or less caused by bad seamen ship; and the marine engineer officer community on the other hand claims that the boiler rules, design and construction are insufficient[18].

Therefore, in line with the pursuit of more exact approximation of the boiler's fatigue lifetime, the recommendation of IIW C-XII could be explored in performing the fatigue life calculations by the use of four linear elastic engineering methods in combination with Paris' Law [13]. Fatigue life analysis assessment method as illustrated in *Figure 2* showed that Linear Elastic Fracture Mechanics (LEFM) would deliver a better result than the Nominal stress method [12].

I. Hot spot stress method
II. Effective Notch stress method

III. Linear Elastic Fracture Mechanics

In addition, with the use of Rigid Body Dynamic (RBD) theory, Six -degree of freedom accelerations of the ship could be accessed and introduce to the Finite Element simulation for the assessment of the fatigue lifetime of the boiler in the marine environment [19].

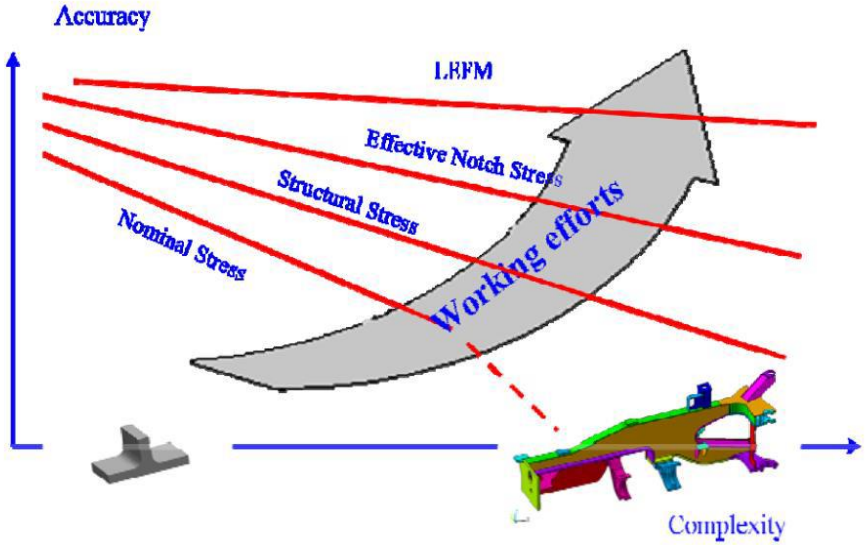

Figure 2: Schematic illustration of fatigue analysis method in relation to accuracy, complexity [4], with author's permission

1.1 Purpose

The purpose of this study is to increase the understanding of how the fatigue lifetime of marine equipment installed aboard floating marine structures is affected by its location of installation.

1.2 Hypothesis

The present author postulates the following hypothesis:

The fatigue life time of a SUNROD CPDB12 marine boiler's critical weld joint can be approximated to a higher confidence by the use of combining RBD, FEA and LEFM compared to the analytical engineering algorithms and equations used by [18].

1.3 Aim and Research questions

The aim of this study is to explore how the fatigue lifetime of the marine boiler design Sunrod CPDB12 is affected by its location of installation by the use of combined RBD, FEM and LEFM simulations; the research question is:

1. To what extent will the fatigue lifetime of a marine boiler with a smallest detectable crack size be influenced of its ship structure allocation?

1.4 Limitations

The thermo-mechanical fatigue life time analyses is limited to the operational load cases, ship dimensions, and the smallest detectable crack used by [18], see *Table 1* and *Figure 3*.

Figure 3. Weld Joint Flaw

Where the Finite Element Analysis (FEA) is limited to the use of the commercial software LS-Dyna and a shell element model.

The following physical phenomena will not be dealt with in this study:

– Fatigue life reduction from oxidation, corrosion and creep
– Transient nozzle load variations
– Mass and forces affecting the nozzles
– Non-linear fracture mechanic (EPFM)
– Material thickness reduction due to wear and tear; and corrosion etc.

Table 1 Essential Data [18]

Sunrod Marine Boiler		Ship	
Operating Pressure [kPa]	800	Length overall [m]	162.5
Maximum Pressure [kPa]	1400	Vessel Width [m]	27.5
Operating Temperature [℃]	200	Block Coefficient	0.74
Steam Boiler Diameter [m]	1.4	Freeboard [m]	13.8
Thickness of Shell [m]	0.012		
Mass of empty Boiler [kg]	7,000		
Mass of water filled boiler [kg]	12,000		
Design Lifetime [Years]	20		
Smallest detectable crack size [mm]	3 x 15		

1.5 Objectives

The objectives of this study are:

I. Review and verification of the results presented in [18]
II. RBD simulation and FEA of the boiler
III. LEFM of the boiler's smallest detectable crack size
IV. Interpretation of simulation results for the boiler's potential deduction of its 20 years design lifetime

1.6 Reliability, validity and objectivity

The results of this study would be benchmark toward the design lifetime of 20 years and the analytical results presented in the work of Castenson and Grandics 2018[18]

2 Scientific Engineering Research Method

The study is performed with the well-established Design for Six Sigma (DFSS) process [20] that constitutes a part of the well-recognised scientific engineering method ‘Systems Engineering’ as defined by:

I. International Council on Systems Engineering Website (INCOSE) [21]-[22].

II. National Aeronautics and Space Administration (NASA) [23]-[24].

III. American Society of Mechanical Engineers (ASME) [25].

Systems Engineering Process is an adopted scientific engineering method for this thesis. It could be defined as an iterative approach of technical evaluation using a well-established Sigma six engineering scientific method for solving problems [22]-[25].

3 Applied Mechanics Methods

3.1 Introduction

The general overall research approach for this study analyses the interaction of thermal and mechanical load cases of steam temperature, pressure, RAO in a system using LS-Dyna FEA commercial software by adhering to the Systems Engineering methods.

Thermo-mechanical fatigue (TMF) is a material deformation developed as a result of the combination of thermal and mechanical loading where both the stresses and temperatures vary with time. It is of higher deformation in order of magnitude which could either be in -phase or out of -phase. Mostly found in start-up and shut-down operational cycles of high temperature components and equipment [5].

3.2 Seakeeping analyses

Seakeeping are general term in marine engineering for sea worthiness of a ship to remain at sea in all conditions in relation to its strength, stability. Engineering variables attached to sea waves are ship's motions, acceleration, speed and power in waves, wetness and slamming which are important variables in fatigue analysis of a marine component [25].

DNVGL rules would be used in determining seakeeping acceleration based on its harmonized well-established theories [26].

Ships are floating body with six degrees of freedom as illustrated in *Figure 6*. The motions of ships are defined as movements and rotations about a set of orthogonal axes through the center of gravity (G). Translations accelerations along the x-y-axes coupled with rotation about the z -axis allows the ship to be in neutral equilibrium. Thus ship/sea system could be regarded as a mass/spring structural dynamics system [28][29]

Seakeeping showed consistently lower RAOs in all waves and at all speeds, the conclusion to be reached would be clear cut. This is not usually the case, and one design will be superior to the other in some conditions and inferior in other conditions of sea waves [19].

Rotational Acceleration on any floating ship structures are the moments around the vertical, transverse and longitudinal axes known as yaw, pitch and roll respectively While translational acceleration are the accelerations of the ship motions around the vertical, transverse and longitudinal axes known as heave, sway and surge respectively.

3.3 Rigid Body Dynamic Analyses

Ship rigid body dynamics are the responses (seakeeping, manoeuvring, structural vibration and dynamism) of a ship during all operational conditions. It could be defined as the excitation response of ship to its motion, acceleration and inertia forces applied during operation in a marine environment [25]

Mathematical, sea keeping theory is a similitude to the linear relationship of ship motions in the six-degrees-of-freedom with respect to sea waves, manoeuvring theory identified the positioning and directional system of COG, COB GM relationship for stability, control, structural vibration and dynamisms in marine world. Therefore, a ship is regarded as a rigid intact body that respond to excitation of its motion and wave amplitudes [28]

In the marine environment, Surface waves flow, it is assumed to be ideal, inviscid, and irrotational in line with the Cartesian co-ordinate system. The center of Buoyancy **(COB)** is a theoretical point though which the buoyant forces acting on the wetted surface of the hull act through. The center of Gravity **(COG)** is the theoretical point through which the summation of all the weights act through. The Metacentre **(GM)** is a theoretical point through which the buoyant forces act. The Metacentric radius **BM** which is the distance between the Metacenter and the center of buoyancy as shown in *Figure 4* [25][28].

During operation ship experiences draft changes thereby creating changes in its Metacenter and center of buoyancy while center of gravity remains on the center line as shown in (*Figure 4-Figure 5*) [25].

The stress and strains caused by the ship motions is approximated by an existing RAO Rigid Body Dynamic FEM-model of the ship; where the boiler can be attached to the xy-rotational plan on the distances to the discretion of the analyser. [Ref Sohail Anwar]

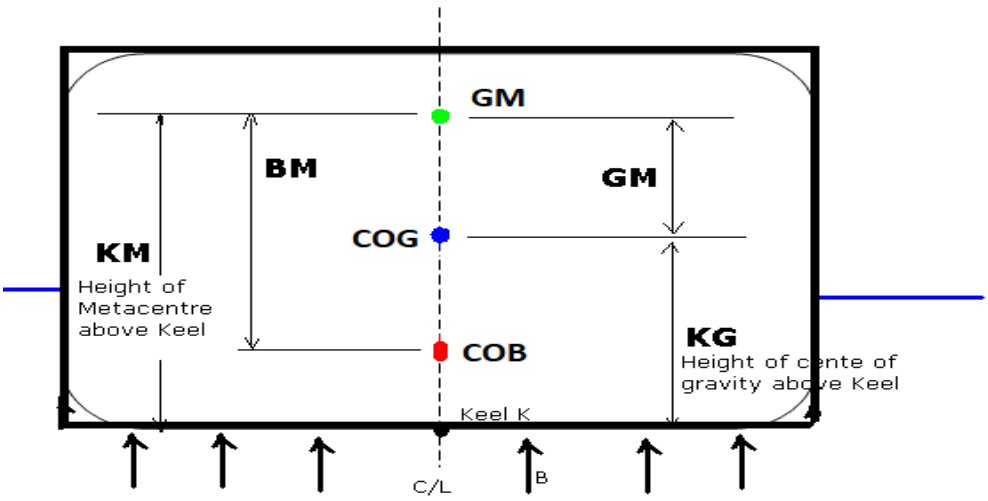

Figure 4: Ship Rigid body dynamics at COG[25].

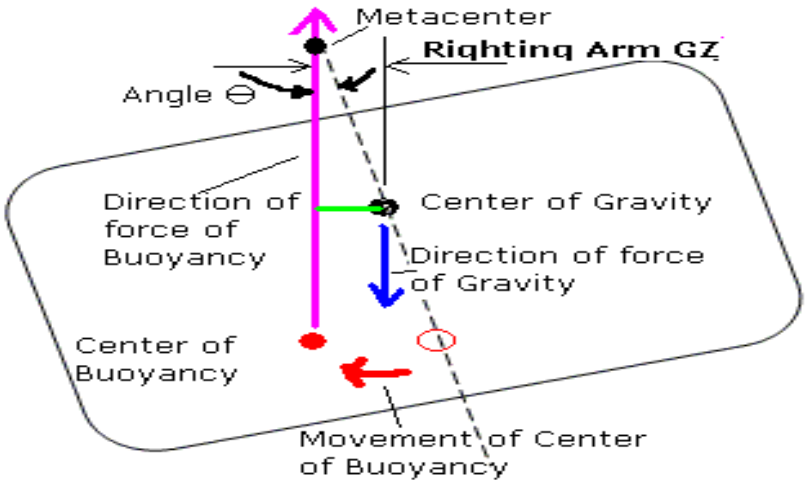

Figure 5: Ship rigid body motion about rotation [25]

Therefore, these accelerations (Rotational and Translational) need to be calculated using DNVGL mathematical relationship shown in equation (1-19) in predicting the fatigue life cycle of the boiler [27].

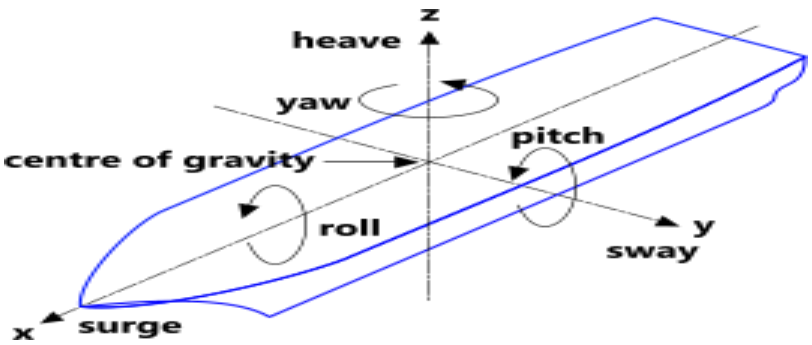

Figure 6. Ship motion and acceleration [27].

$$a_o = \left(1.58 - 0.47CB\left(\frac{2.4}{(\sqrt{L})}\right) + \left(\frac{34}{(L)}\right) - \left(\frac{600}{(L)^2}\right)\right) \quad (1)$$

$$a_{heave} = \left(1.15 - \left(\frac{6.5}{(\sqrt{g * L})}\right)\right) fpa_0 g \quad (2)$$

$$a_{heave} = \left(1.15 - \left(\frac{6.5}{(\sqrt{g * L})}\right)\right) fpa_0 g; \quad (3)$$

$$a_{surge} = 0.2 * \left(1.6 + \left(\frac{1.5}{(\sqrt{g * L})}\right)\right) * fp\ a_0 g; \quad (4)$$

$$a_{sway} = 0.3 * \left(2.25 + \left(\frac{20}{(\sqrt{g * L})}\right)\right) * fp * a_0 * g \quad (5)$$

$$a_{roll} = fp * Roll_{angle} * \left(\frac{\pi}{180}\right) * \left(\frac{2\pi}{Roll_{period}}\right)^2 \quad (6)$$

$$Roll_{period} = 2.3 * \pi * \left(\frac{kr}{(\sqrt{g * GM})}\right) \quad (7)$$

$$Roll_{angle} = 9000 * (1.4 - (0.035 * roll_{period}) \left(\frac{fp * fbk}{(1.15 * w) + 55}\right) * \pi \quad (8)$$

$$a_{pitch} = 0.8 * (1 + 0.05 * v) * fp * \left(0.72 + \left(2 * \frac{L}{700}\right)\right) * \left(1.75 - \frac{22}{(\sqrt{g * L})}\right) * P_{angle} * \left(\frac{\pi}{180}\right) * \left(2 * \frac{\pi}{P_{period}}\right)^2 \quad (9)$$

$$Pitch_{period} = \sqrt{\frac{2.3 * \pi * \lambda}{g}} \quad (10)$$

Wavelength $\lambda = 0.6 * (1 + fT) * L$ (11)

$$Pitch_{angle} = 920 * fp * L^{-0.84} * \left(1 + \left(\frac{2.57}{(\sqrt{g * L})}\right)^{1.2}\right) \quad (12)$$

Correction Factor Based on vessel Speed (13)

$$f_v = 0.2 * v * -0.105 + (0.12) * \left((z - \frac{0.875 * TLC}{TLC}\right)$$

$$a_{pitch\ X} = a_{pitch} * (z - R)$$

$$a_{roll\ Y} = a_{roll} * (z - R)$$

$$a_{Picth\ Z} = a_{pitch} * (1.08 * X) - (0.45 * L)$$

Total Acceleration X-Direction (14)

$$a_y = \left(1 - e^{-\frac{W*L}{215GM}}\right) * \left(\left(a_{sway}\right)^2 + g * \sin\left(Roll_{angle} * \left(\frac{\pi}{180}\right) + (a_{roll\ Y})^2\right)\right)$$

Total Acceleration Y-Direction (15)

$$a_y = \left(1 - e^{-\frac{W*L}{215GM}}\right) * \left(\left(a_{sway}\right)^2 + g * \sin\left(Roll_{angle} * \left(\frac{\pi}{180}\right) + (a_{roll\ Y})^2\right)\right)$$

Total Acceleration Z-Direction *(16)*

$$a_z = \left((a_{heave})^2 + 0.95 + e^{-\frac{L}{15}} * (a_{Picth\ Z})^2 + (1.2\ a_{roll\ Z})^2\right)$$

Stress in X-Direction *(17)*

$$\sigma_x = \left(\frac{M * a_x}{Area}\right)$$

Stress in Y-Direction *(18)*

$$\sigma_y = \left(\frac{M * a_y}{Area}\right)$$

Stress in Z-Direction *(19)*

$$\sigma_z = \left(\frac{M * a_z}{Area}\right)$$

3.4 Linear Elastic Fracture mechanics

Fracture mechanics that deals with a cracked structure, can be traced back to Griffith when he explored the first law of thermodynamics to a stressed plate of an elastic material when a crack was introduced, it was observed that a flaws/ cracks created or existing crack growth was due to change between the potential energy and surface energy of the cracked surface area that tends to be in equilibrium. It is known as the energy balance of the crack area under equilibrium [30].

Inglis observed that Stress concentration variation between the actual strength and theoretical strength estimate of a material was due to flaws when a plate was subjected to an applied stress perpendicular to the major axis of the crack. The global stress of the flaws at the tip of crack was magnified by the local stresses, thereby accounted for failure [30].

Irwin presented a modified Griffith's energy criterion. He defined energy balance relationship between thermodynamic driving force (stored elastic strain energy which is released as a crack grows) and thermodynamic resistance (dissipated energy which includes plastic dissipation and the surface energy) drift towards equilibrium which accounted for as for crack growth [30]. Therefore, Crack growth theories has been a basis for fracture mechanics

Fracture approach do estimate total fatigue life of a structural component from crack initiation phase to a through-penetration phase. It has been widely used is estimating crack propagation life of a fatigue -induced crack in ship and offshore structures [31].

There are three independent loading modes in fracture mechanics of a mechanical component subjected to crack propagation are namely; Mode I, II and III as shown in *Figure 7* [32].

Mode I is the crack opening mode where the crack surfaces move apart and is the most common loading type.

The Mode II is an in- plane shear mode where the crack surfaces slide apart perpendicular to the crack.

Mode III is an out-of-plane shear mode where the crack surfaces slide apart in a tearing manner. A cracked body can be loaded in any of these modes or combination of two or three mode.

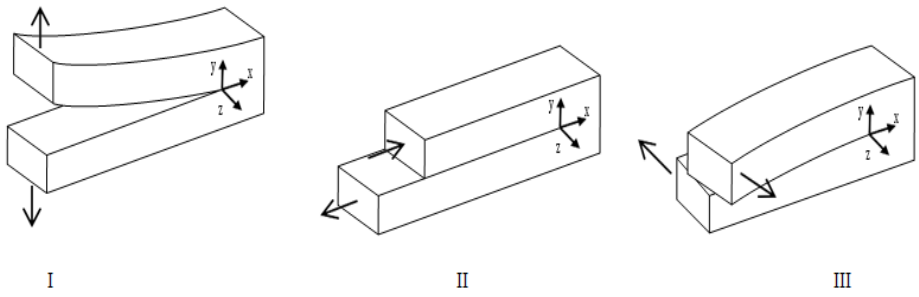

Figure 7. Loading modes for cracks [30]

The stress components are equation 20 [30]:

$$\sigma_{ij} = \sigma_{ij}{}^{1} + \sigma_{ij}{}^{2} + \sigma_{ij}{}^{3} \qquad for\ \ i,j = x,y \qquad (20)$$

Irwin expressed the behavior of the stress component to the crack tip (r) within the scope of linear elasticity theory [32]

For a linear elastic material, the stresses and displacements are considered in Mode 1 tensile loading for crack growth analysis as shown in *Figure 8*[30].

3.4.1 Model 1-Stresses and Displacements

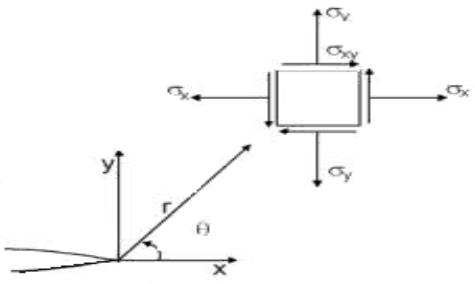

Figure 8.coordinate system of the stress field at the tip of a crack [32]

The stress distribution in the region near tip of the crack equation 21 [32]:

$$\sigma_{ij}(r\theta) = \frac{k_1}{\sqrt{2\pi r}} {f_{ij}}^1(\theta) + \frac{k_2}{\sqrt{2\pi r}} {f_{ij}}^2(\theta) + {\sigma_{ij}}^0 \ + O\left(\sqrt{r}\right) \quad (21)$$

$$for\ r \to 0, and\ i,j\ = x,y, {\sigma_{ij}}^0 - finite\ crack\ at\ the\ crack\ tip.$$

For model I, stress intensity factor equation 22 [32]

$$k_1 = \lim_{r\to 0}\left(\sqrt{2\pi r}\sigma_{ij}(r\theta)\right) \quad (22)$$

The angular variation function for mode 1 are equation 23-25 [32]:

$${f_{xx}}^1(\theta) = cos\left(\frac{1}{2}\theta\right)\left(1 - \left(sin\frac{1}{2}\theta\right)\right) sin\left(\frac{3}{2}\theta\right) \quad (23)$$

$${f_{yy}}^1(\theta) = cos\left(\frac{1}{2}\theta\right)\left(1 + \left(sin\frac{1}{2}\theta\right)\right) sin\left(\frac{3}{2}\theta\right) \quad (24)$$

$${f_{xy}}^1(\theta) = cos\left(\frac{1}{2}\theta\right)\left(sin\frac{1}{2}\theta\right) sin\left(\frac{3}{2}\theta\right) \quad (25)$$

The Displacement field near the crack tip, equation 26 [32]:

$$u_i(r,\theta) = {u_i}^0 + \frac{k_1}{u}\sqrt{\frac{r}{2\pi}}\bar{f_i}^{\,1}(\theta) + \frac{k_1}{u}\sqrt{\frac{r}{2\pi}}\bar{f_i}^{\,2}(\theta) \ + O\left(\sqrt{r}\right) \quad (26)$$

$$for\ r \to 0, and\ i,j\ = x,y, {u_i}^0 - crack\ tip\ displacement$$

The angular variation functions are equation 27-28 [32]:

$${f_x}^1(\theta) = cos\left(\frac{1}{2}\theta\right)\left(\frac{1-v}{1+v} + \ sin^2\left(\frac{1}{2}\theta\right)\right) \quad (27)$$

$${f_y}^1(\theta) = sin\left(\frac{1}{2}\theta\right)\left(\frac{2}{1+v} + \ cos^2\left(\frac{1}{2}\theta\right)\right) \quad (28)$$

Model 1 linear elastic fracture mechanic characterization of stress and displacement in the vicinity of crack tip [32].

3.5 Fatigue crack growth

Fatigue crack due to flaws is defined as progressive and localized structural damage that occurs when a material is subjected to loading. It do start with the nucleation of grains in the microstructure constituent of the material, dislocation and movement of grains along the microstructural boundary thereby creating crack. The crack created could either grow or inhibited along the grain boundary with microstructure barrier within the material [32].

The three stages of crack growth are [34]:

- Stage 1 as Crack initiation. Fatigue cracks initiated through the release of shear strain energy of either a uniform or sinusoidally varying forces (around pores, inclusions or impurities, unsmooth surfaces) which result into local deformation along slip planes or slip bands with an embryonic crack approximately 1 to 10 microns in height. A crack initiated reaches the grain boundary, then gradually transferred to the adjacent grain. When the crack has grown through approximately 3 grains, it changes its direction of propagation towards maximum shear plane, or 45 degrees, to the direction of loading.
- Stage 2 as crack growth or propagation. The crack is sufficiently large to form a geometrical stress concentration. A tensile plastic zone is created at the crack tip and the crack propagates perpendicular to the direction of the applied load.
- Stage 3 as Fracture, when a crack grows to a critical size, at which the structure is not able to withstand the next cyclic load, fracture occurs.

Fatigue crack propagation analysis could be done either using the mesoscale crystal plasticity-based approach where the individual properties -size, direction and location are the baseline for the analysis or the continuum-based approach where strain, stress and fracture mechanic system could be adopted. Fracture mechanics approach has been proven adopted method for analysing the structural integrity behaviour of flaws at various welding joints of a mechanical component [34][35].

3.6 LEFM and cycling Loading

A mechanical component that are subjected to cyclic Loading histories can be defined as shown in *Figure 9*. Cyclic loading being a non-permanent load, fatigue estimation is usually based on stress range or stress intensity factor range which are calculated from the superposition of all the loads during the anticipated service life of the structure [31].

For this analysis, stress range would be used for the fatigue assessment of the cyclic loading as expressed in equation 29-33

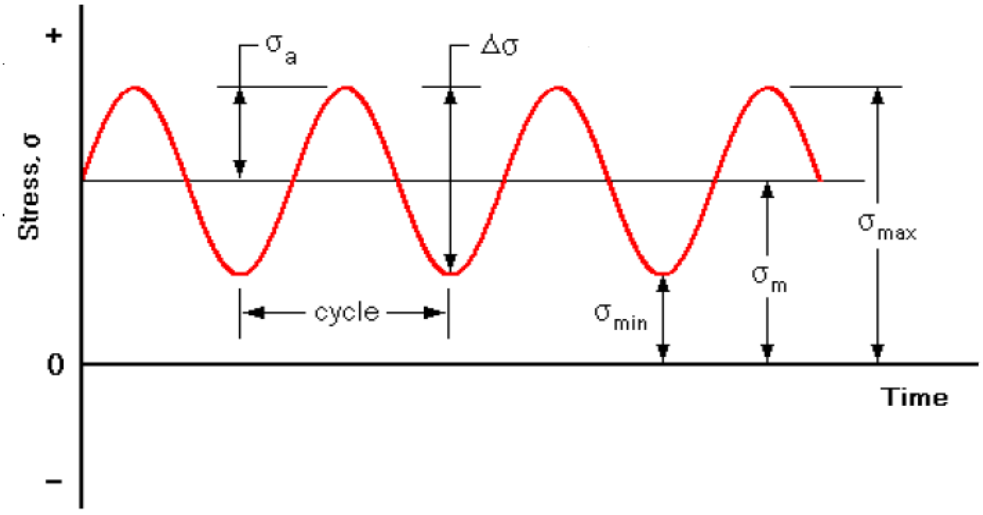

Figure 9: Cyclic loading [31]

$$\sigma_a = \frac{\Delta\sigma}{2} \qquad (29)$$

$$\Delta\sigma = \Delta\sigma_{max} - \Delta\sigma_{min} \qquad (30)$$

$$\sigma_m = \frac{\Delta\sigma_{max} + \Delta\sigma_{min}}{2} \qquad (31)$$

$$\sigma_{max} = \sigma_m + \sigma_a \quad , \quad \sigma_{min} = \sigma_m - \sigma_a \qquad (32)$$

$$R = \frac{\sigma_{max}}{\Delta\sigma_{min}} \quad , \quad A = \frac{\sigma_a}{\sigma_m} \qquad (33)$$

3.7 Paris Law

Paris and Erdogan described fatigue crack growth behaviour in a metallic material is mainly control by the range of stress intensity factor (ΔK) [36]**Error! Reference source not found.**. The experimental relationship between the fatigue growth rate ($\frac{da}{dN}$) and stress intensity factor range (ΔK) in a sigmoidal curve log- log plot as illustrated in *Figure 10* with three distinct regions (1, 2, 3) [37].

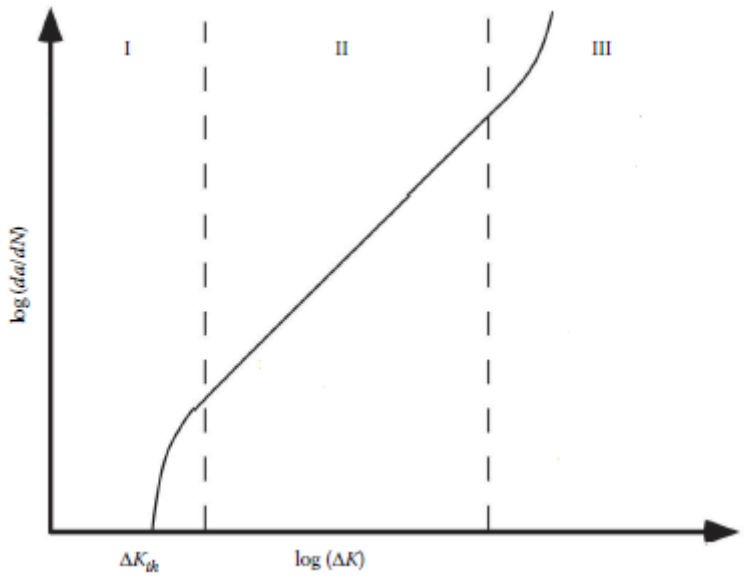

Figure 10. Crack growth curve [36]

Region 1, the stress intensity factor range is below the threshold (ΔK_{th}) with no crack growth occurs because the crack growth is being arrested by the micro-structure boundaries.

Region 2: exhibits stable fatigue crack growth with linear relationship with Paris power growth.

Region 3: represent rapid crack growth at the increasing growth where the linear relationship of the Paris law has been defeated, thereby fracture occurs at this stage.

The stress intensity factor mathematical relation of Paris law are equation 34-36 [32][39]:

$$\textit{Stress Intensity Factor}\ \Delta K_1 = \Delta K\ = K_{max} - K_{min} = \Delta\sigma_{max}\ -\ \Delta\sigma_{min} \qquad (34)$$

$$\textit{Generalized Paris power law}\qquad \frac{da}{dN} = C\Delta K^m \qquad (35)$$

Modified Paris Power law $\frac{da}{dN} = C(\Delta\sigma)^m$ *(36)*

The estimate of fatigue life can be made by integrating the Paris crack growth law, for the SIF range within the region 2, the linear region equation 37 [39]:

$$\int_{N_o}^{N_i} dN = \int_{a_o}^{a_i} \frac{da}{C(\Delta\sigma)^m} \quad (37)$$

Equation 27 can be used to determine fatigue cycles, $N_f - N_o$ that are required to propagate the crack (a_o) from the initial stage to reach a certain size (a_f).

The Euler integration of equation 38-39 [32][39].

$$N_{m+1} = N_m + \frac{\Delta a}{C[\Delta\sigma\,(a_m)]^n} \qquad (m = 0,1 \ldots\ldots n) \quad (38)$$

$$a_{m+1} = a_m + C[\Delta\sigma\,(a_m)]^n \Delta N \qquad (m = 0, \quad) \quad (39)$$

3.8 Palmgren-Miner's Rule

Palmgren-Miner linear damage (D) defined the relationship between the number of load cycle (n_i) to pertinent fatigue life load cycles (N_i) of a mechanical loading history of a component. Fatigue failure would occur when the ratio between (n_i) and (N_i) is unity [32] as shown in Equation 40. The fatigue lifetime (T_d) is define in Equation 41.

$$D = \sum_{i=1}^{k} \frac{n_i}{N_i} = 1 \quad (40)$$

$$T_d = \frac{1}{D} \quad (41)$$

Where D is experimentally found to be between 0.7 and 2.2. The most common approach to fatigue analysis because of its simplicity, effectiveness, and its accuracy is good enough in many applications [31].

4 Identification of the load cases

4.1 Introduction

The author is only considering the wave-induced loads used by carstenson & Grandics for three (3) different locations of boiler installation, as illustrated in the *Figure 11*, namely:

I. Ship's centre of rotation, which is presumed to be identical to the ship's centre of buoyancy as *load Case-I*
II. On the ship' engine room tank top (y = 5 m; Z = - 65 m) *Load Case-II*
III. In the top of the ship's funnel (y = 17 m; Z = - 65 m) Load *Case-3*

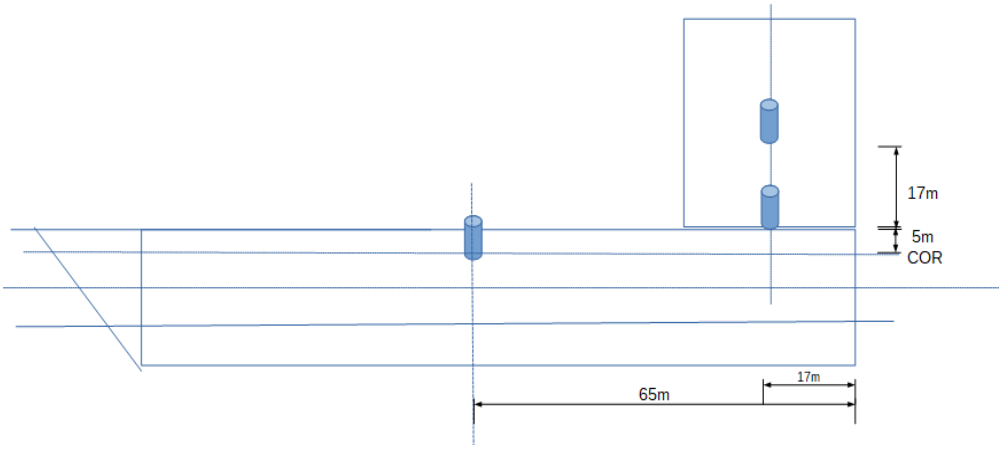

Figure 11.load Case and different loading Condition.

4.2 Response amplitude operator load cases

Response amplitude operator load cases (RAO) defines the movement of a floating vessel in six degrees of freedom: Surge, Sway, Heave, Roll, Pitch, and Yaw in a marine environment due to a passing hydrodynamic wave. RAOs are engineering variables of displacements, accelerations, and velocities at any given location on a marine vessel as well as that imposed forces on structures and/or equipment. The linear movements in the x, y, z directions (Surge, Sway, and Heave) and rotary movements about the x, y, z axes (Roll, Pitch, and Yaw), respectively. The computed RAO data for the 3-load cases are shown in *table 2*.

Table 2: RAOs at the centre of Rotation

S/No	RAOs	*Centre of Rotation*
1	a_{surge} [m/s^2]	0.855
2	a_{heave} [m/s^2]	2.578
3	a_{Sway} [m/s^2]	1.370
4	a_{roll} [Rad/s^2]	0.052
5	a_{yaw} [Rad/s^2]	0.00
6	a_{pitch} [Rad/s^2]	0.103

4.3 Thermal Load cases.

Thermal loading are steam temperature distribution in a boiler. During operation, a transient thermal gradient occurs during heat-up and cool-down cycles where the thermal gradient is changing with time. During operation with a steady heat input inside a fire-tube chamber the heat distribution will be logarithmic between the inside and outside of the Tube due to thickness of the vessel wall. While linear temperature distribution occurs at the external wall of the marine boiler.

4.4 Pressure load cases

Internal or external pressure contribution during operation and hydrostatic head of water in a marine boiler. Pressure load could be (steady, on -steady, variable, or temporary) over a large portion (general area) of the vessel or Over a local area of the vessel. In a Marine boiler, pressure loading are longitudinal, Circumferential and tensional on the inside surface of the vessel, and compressive on the outside. For steady loads during operation, the boiler must support these loads continuously during its useful life while non-steady loads occurred during periodic start up, shunt down and maintenance of the vessel.

5 Analyses

5.1 Finite Element analyses

The Author used the commercial FEM software LS-DYNA to perform numerical analysis of the Marine boiler. The code's origins lie in highly nonlinear, transient dynamic finite element analysis using implicit time integration responses to: Changing boundary conditions, deformations, transient dynamic and non-linear materials that do not exhibit ideally elastic behavior [38].

Finite Element Method (FEM) simulation would be used in analysing Linear Elastic fracture mechanics (LEFM) of the boiler due to thermo-mechanical loading and its fatigue life cycle with a user friendly graphical interface for the assessment of structural integrity in the general boiler's design with respect to the smallest detectable flaws at the welding joint [17] and [33].

5.2 Geometry with meshing of the model.

The model's geometry with dimensions are shown in *Figure 12*. The Shell domains were build-up with 14 parts. Shape Mesher tool with both triangular and quadrilateral elements was used. The element sizes were 20mm in all directions having 35,379 elements and 36,296 nodes for the boiler domains. This element size was considered to be the smallest size with acceptable computational time mostly for fast running accurate simulation as shown in *Figure 13*

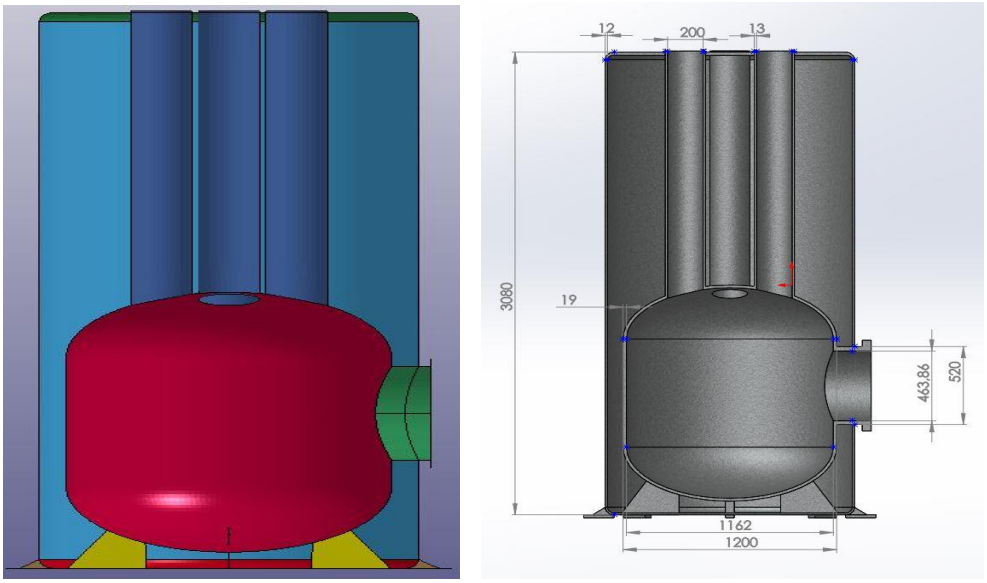

Figure 12.FEM Model with Dimensions

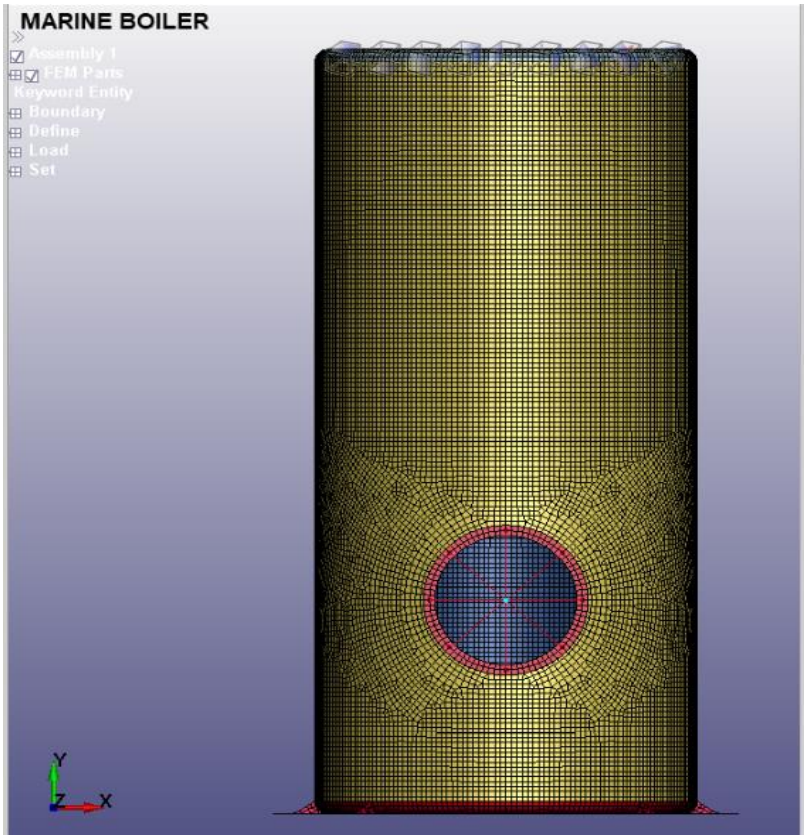

Figure 13.Meshed Model

5.3 Boundary Conditions

Boundary conditions are all physical phenomena acting and/or reacting on a structure, thereby subjecting all structures to response to thermal, mechanical or thermo-mechanical excitation. Nevertheless, for the sake of simplicity some structural analysts prefer to mention some B.C. as loads and some for B.C. But in a physical sense they are all B.C. [Ref P. Lindström private communication]

The present authors have identified that the marine boiler is subjected to the following mechanical boundary conditions:

- Gravity and ship motion reaction forces in the boilers support points
- Thermal expansion and contraction as a function of the fluids' temperature variations
- Gravity variation as a function of the boiler water level and water temperature
- Boiler water and steam pressure variations
- The ship motion reaction forces are by convention given in the form of acceleration values were denoted as Response Amplitude Operators, (RAO).

5.3.1 Pressure Load

Identification and quantification of Cyclic loading due to Pressure boundary conditions could be defines as the stresses (constant or varying amplitude during operation) as a result of the changing temperature thereby accounted for pressure variation within the system.

5.3.2 Thermal Load

The present authors have identified that the marine boiler is subjected to the following thermal boundary conditions**.**

- Internal surface (boiler water and steam temperature variations)
- External surface (Heat transfer from boiler to surrounding atmosphere by convection and radiation)
- Conduction heat transfer across contact surfaces
- Heat flux between the exhaust gas on the inner surface of the tube and firebox.

5.3.3 RAO Load

Response Amplitude Operator (RAO), Seakeeping Analysis boundary conditions were significant to the geometry of a ship and its motion. The momentum conservation principles of the ship responded to the wave's propagation of the sea with respect the ship motion, thereby causing excitation responses of the marine boiler.

The authors adopted DNVGL modelled mathematical relationship (Equation 31-50) for the computation of the Response Amplitude Operator (RAO) for the three load cases.

5.3.4 Linear Elastic Material data

A Normalized Steel plate material (St 52-3) steel plate material data is used in this study as stated in *Table 4* [33].

Table 3: Normalized Steel Plate (St 52-3) material data

S/No	Mechanical Properties	0 ℃	500 ℃
1	Mass Density [kg/m^3]	7800	
2	Young's Modulus of Elasticity [MPa]	210	175
3	Poisson ratio	0.30	0.31
4	Tangential Coefficient of Thermal Expansion [1/℃]	2.25E-05	1.90E-05
5	Tensile Strength, Yield [MPa]	420	230
6	Plastic Hardening Modulus [GPa]	1.150	1.050

5.4 Cycle Counting – Rain flow Method.

Cycle counting is the process of converting a variable amplitude stress sequence into a series of constant amplitude stress range cycles that are equivalent in terms of damage to the original sequence. Rain flow method of counting for the stress-time history are done by rearranging the history to start with either highest or lowest valley. The highest peak goes down to the next reversal, the continuous rain flow runs down and continue unless the magnitude of the following peak is equal to or greater than the peak from which it was initiated. The procedures continuous for subsequent peak and valley point.[12] [32]

The Rain flow cycle counting of the FEA simulation result were explored in delivering constant amplitude Stress range of each load cases.

5.5 Fatigue crack growth analyses

Introduction

The fatigue crack growth was analysed for a subsurface crack just below the outer shell surface in one of the boiler's longitudinal weld seams as illustrated in the *Figure 14* with the crack size is 3 mm deep and 15 mm long

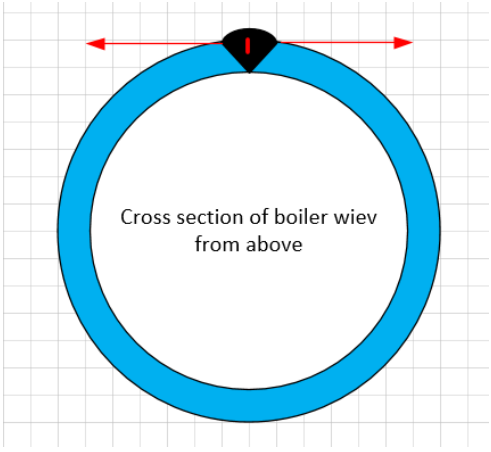

Figure 14: Crossection of crack on the boiler

For stage 1 crack growth, it would not possible to estimate or calculate the crack growth at initiation stage because it is an inbuilt within the manufacturing process. A numerical method for this type of crack initiation simulations have recently been proposed by [33].

Fatigue analysis for stage 2 would be enumerated using stress range and Palmgren damage relationship [39][40].

The stress range ($\Delta\sigma$) results gotten from Rain flow cycle counting of the FEA simulation loading history are post processed to obtain the fatigue cycles number (n_i)of each load case. For this analysis, the adopted crack shape (Double Butt Weld with a Toe Crack in Tension)

A fatigue crack growth analysis would be carried out using the following data:
Initial Crack size(a_1) $= 3\text{mm}$
Final Crack size $(a_f) = 10\text{mm}$ the half wall thickness of the boiler.
Crack growth parameters size $C = 8.2 \times 10^{-13}$, m =3.6
Crack Stress Intensity threshold parameters $\Delta k_{th} = 0$ according to BSN Standard in the marine environment.
Stress ranges $\Delta\sigma$ accordingly to each load cases at location 1, 2, 3 respectively
The Fatigue life cycle number (n_i) of each load case were obtained.

5.6 The Palmgren-Miner Rule

The Stress range S-N curve of IIW standard with benchmark expected number of cycles ($N_f = 10^7$) were related to the obtained number of cycles to failure (n_i) for each load case were analysed using palm gren equation in order to obtain correspond fatigue life in relation to the 20 years design life of the marine boiler .

The Fatigue life Td were obtained using equation 40-41.

IIW recommended [31] suggested that palm green damage sum of ($D = 0.10$) for a welded steel joint under variable amplitude loading with constant stress but for a wider Branded spectrum of mean stress($D = 0.2$).

The result obtained were the bases for discussion and answering the research question.

6 Result

Introduction:

The numerical simulation of each location with its graphical interface are shown in *Figure 15*. The Maximum principal stress and spot identified as the smallest detectable cracks were analysis at the different location using rain flow counting method for each load case.

6.1 Results of the parametric transient FEA result

The results of the parametric FEA simulations where extracted from exactly the same spot for all three simulations i.e. Boiler at ship hull location 1, 2 and 3; see *Figure 15*

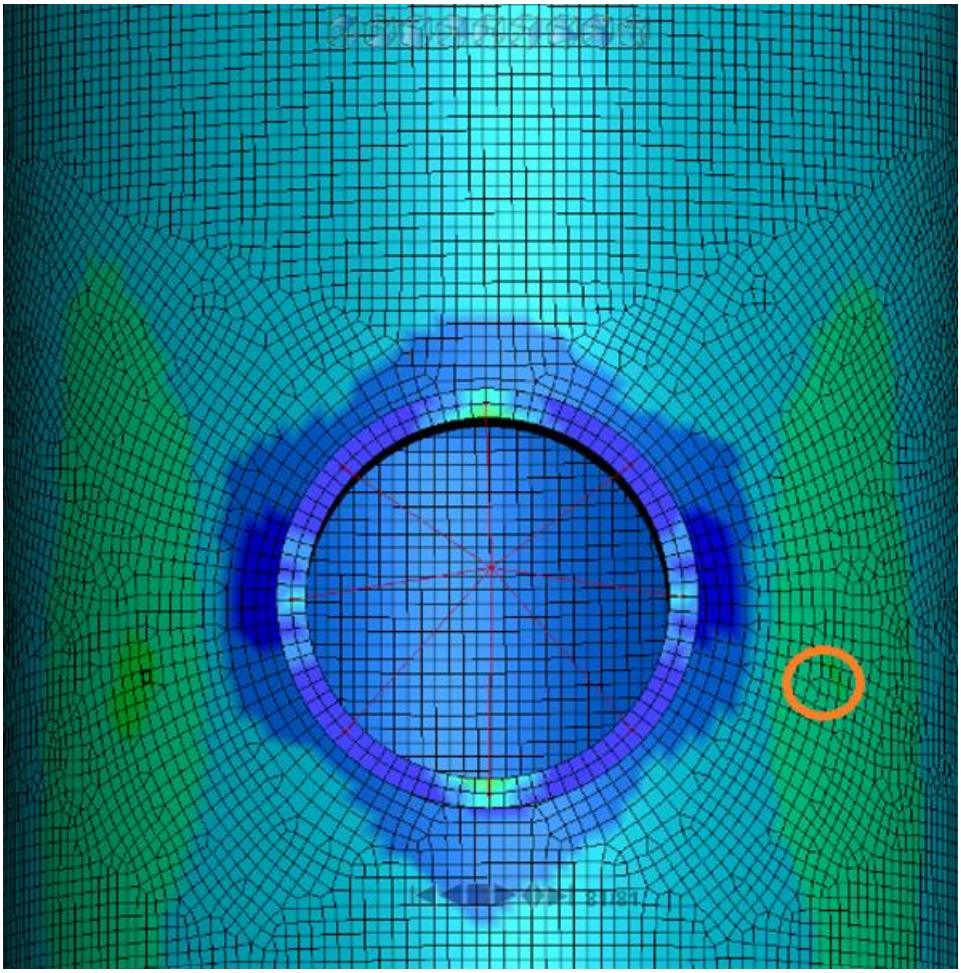

Figure 15: Illustration of stress and strain affected boiler region assessed

6.2 Rain flow cycle of the FEA result

The Maxima principal stress obtained from numerical simulation for each load case were recorded for analysis using rain flow cycle method of the stresses. The stress range were calculated accordingly using equation 30 for the 3 locations. The results are shown in *Table 4.*

Table 4: Load cases at location 1,2,3

Load cases	Location 1	Location 2	Location 3
LC 1 $\Delta\sigma$ [MPa]	114.09	114.09	109.36
LC 2 $\Delta\sigma$ [MPa]	15.69	15.69	14.88
LC 3 $\Delta\sigma$ [MPa]	0.08	0.010	0.075
LC 4 $\Delta\sigma$ [MPa]	0.04	0.06	0.053
LC 5 $\Delta\sigma$ [MPa]	0.09	0.13	0.117
LC 6 $\Delta\sigma$ [MPa]	0.25	0.25	0.155
LC 7 $\Delta\sigma$ [MPa]	0.17	0.17	0.1066
LC 8 $\Delta\sigma$ [MPa]	6.60	35.37	164.60

6.3 Crack growth results

Crack growth analysis using linear elastic fracture mechanics for the identified crack defect in Tension at the welding Joint as a double butt Weld with a Toe Crack in the boiler. The results of cycles to failure (N_f) of each load case are shown in (*Figure 16-Figure 20*).

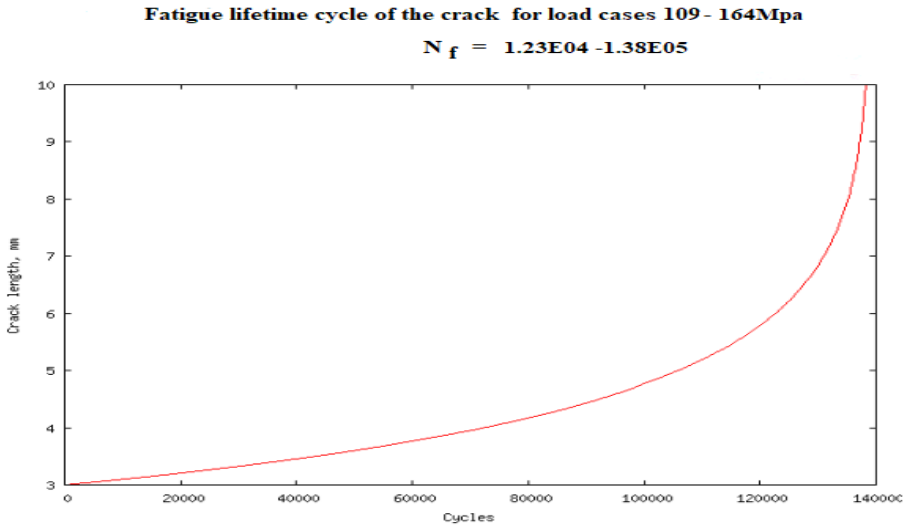

Figure 16: load case 109-112MPa

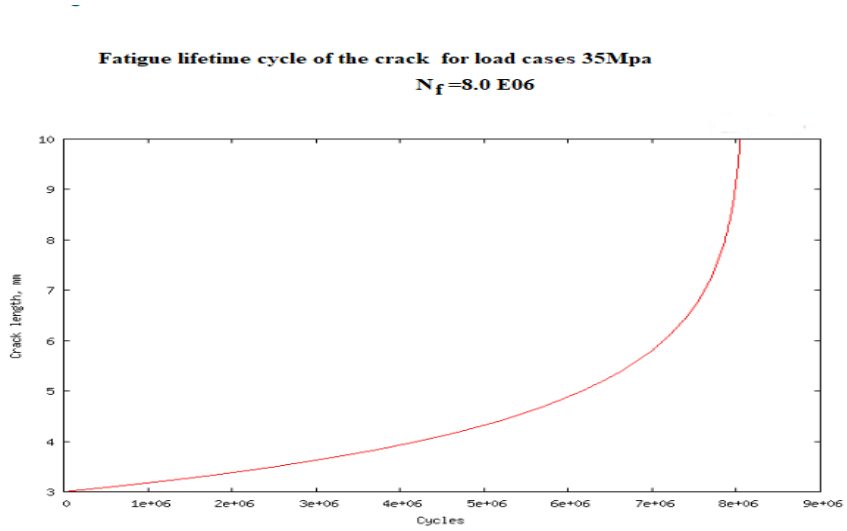

Figure 17: load case 35.5MPa

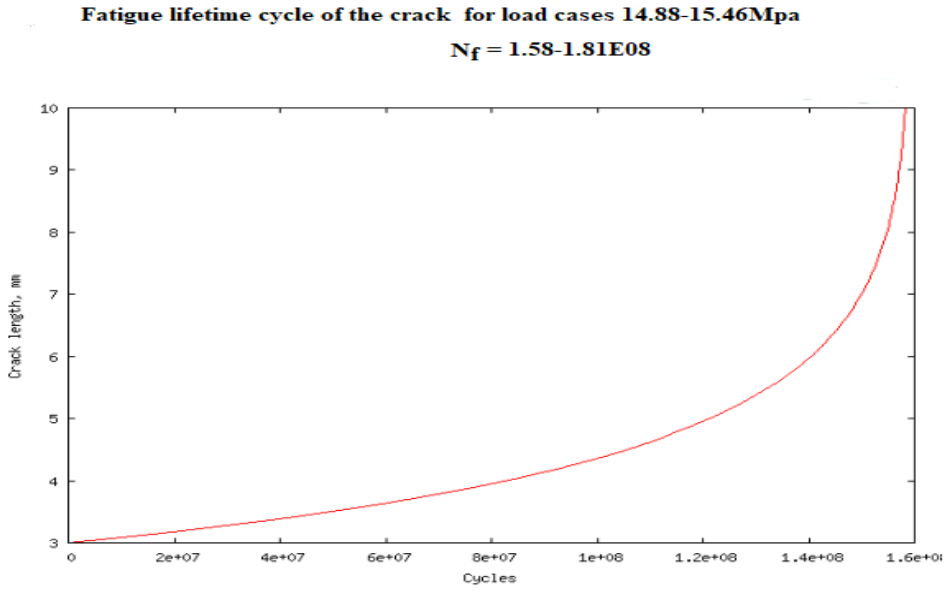

Figure 18: load case 15MPa

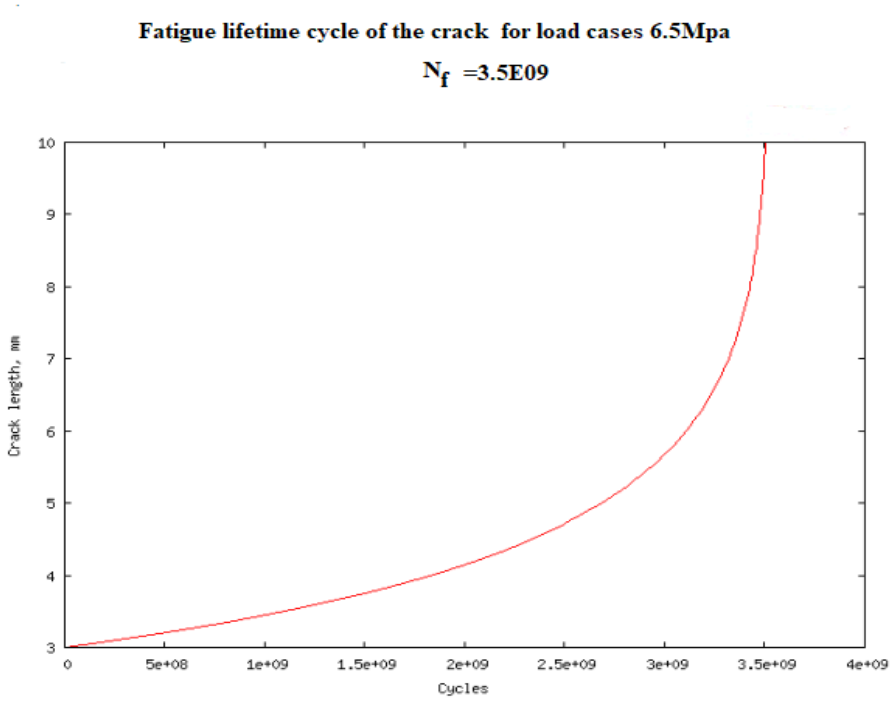

Figure 19:load case 6.5MPa

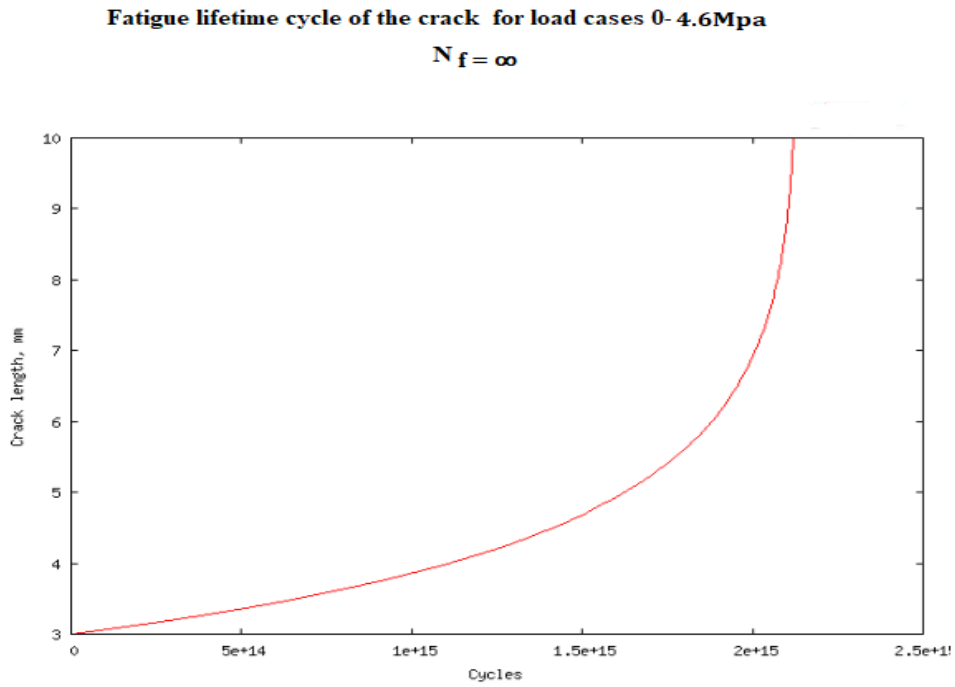

Figure 20:load Case 0.08-4.65 MPa

6.4 Palmgren-Miner linear damage

Palmgren-Miner linear damage fatigue failure analysis of the marine boiler at each load case using equation 30- 31.

According to *Table 5- 7*, fatigue failure as a result of these crack propagation were estimated for each location as cumulative sum of the individual load case contribution.

Also, *Table 8*, had it that 12.94, 3.46 and 0.12 years are the fatigue lifetime estimated for the 3 location respectively.

It could be inferred that the locational position of boiler do affect the fatigue life of welded Joint.

Table 5: Palm gren -Miner analysis for location 1 using load case 1-8

Location 1	N_i	N_f	D_{lc}	$D_{20\,total}$	T_d
LC 1	1.2E03	1.2E05	0.010	0.077	12.94
LC 2	1.0E07	1.50E08	0.067		
LC 3	1.7E06	0.0E00	0		
LC 4	1.7E06	0.0E00	0		
LC 5	1.7E06	0.0E00	0		
LC 6	1.7E06	0.0E00	0		
LC 7	1.7E06	0.0E00	0		
LC 8	1.7E06	3.5E09	0.0005		

Table 6: Palm gren -Miner analysis for location 2 using load cases 1-8

Location 2	N_i	N_f	D_{lc}	$D_{20\,total}$	T_d
LC 1	1.2E03	1.2E05	0.010	0.289	3.46
LC 2	1.0E07	1.50E08	0.067		
LC 3	1.7E06	0.0E00	0		
LC 4	1.7E06	0.0E00	0		
LC 5	1.7E06	0.0E00	0		
LC 6	1.7E06	0.0E00	0		
LC 7	1.7E06	0.0E00	0		
LC 8	1.7E06	8.0E06	0.212		

Table 7: Palm gren -Miner analysis for location 3 using load case 1-8

Location 3	N_i	N_f	D_{lc}	$D_{20\,total}$	T_d
LC 1	1.2E03	1.3E05	0.008	54.6	0.12
LC 2	1.0E07	1.6E08	0.055		
LC 3	1.7E06	0.0E00	0		
LC 4	1.7E06	0.0E00	0		
LC 5	1.7E06	0.0E00	0		
LC 6	1.7E06	0.0E00	0		
LC 7	1.7E06	0.0E00	0		
LC 8	1.7E06	8.0E06	54.10		

Table 8: Palm gren -Miner analysis of the location in summary

Location	Cumulative Palmgren damage (D)	Fatigue life in Years (T_d)
1	0.077	12.94
2	0.289	3.46
3	54.6	0.12

7 DISCUSSION

The author has performed a linear finite element analyses of a Marine boiler-Sunrod CPDB12 with 24 load cases and benchmarking the result with available standards - IIW, DNVGL, BSN codes. The FEM models of the boiler was built with its geometry, meshed, loaded thermally and mechanically using linear elastic material (steel).

LEFM analysis of crack growth of the welding flaws for three location were analysed using the scientific system engineering method with numerical simulation for post processing analysis of the data.

The recalculation task of the BSc thesis data, it was observed that some computation errors were recorded on the RAO but it has being corrected in line with DNVGL rules. It could be inferred that the numerical FEA delivered more accuracy.

The stress range for each load case were recorded. It was observed the crack would not grow at lower stress range (0.08- 4.689 MPa) load cases across board, thereby making the fatigue life to be at infinity. However, load cases with higher stress range are proportional to the crack growth curve as shown in table 5-8.

The rain flow stress range counting as shown in *Table 4* for various location, it could be inferred that location of the boiler's installation do account for growth of the stress range, thereby adversely affecting the fatigue life of the boiler.

With palm gren analysis, it could be inferred that flawless boiler would fulfil the design safe life of 20 years. On the other hand, damage created by the smallest detectable crack has reduced the designed safe life of 20 year to 12.94, 3.46 and 0.12 at location 1,2,3 respectively. Therefore, welding flaws size have a large effect on the fatigue crack growth (life) of the boiler.

8 CONCLUSION

This Thesis, a series of conclusions were made on fatigue crack growth using linear elastic fracture mechanics. A numerically investigation of the fatigue crack growth of the smallest detectable weld flaws identified by [18] in a marine boiler Sunrod CP 20. The fatigue life prediction of the crack growth, under mode 1 loading was examined using FE simulation technique. The numerical accuracy of this technique was examined, particularly by comparing with the exact solution of the analytical computation done by BSC thesis and available standards.

The following principal conclusions are drawn:

- The accuracy of fatigue crack growth rate assessments and life predictions are heavily dependent on the installation location of the boiler.
- Based on the result of this study's analyses for a case with a smallest detectable flaw in a critical welding joint of the boiler, the 20 Years design lifetime of the boiler has being reduced to:
  I. 13 years, at location 1
  II. 3 years, at location 2
  III. 2 months at location 3
- Location 1 appeared to be a better location for the installation of the boiler.

9 Recommendations

With the analytical and numerically investigation of the fatigue life of marine boiler Sunrod CP 20. The corrosion engineering variable could be integrated into the analysis of the fatigue life of the boiler for a complete overview of the situation.

References

[1] Stone, Joe, 2015, Floating Palaces of the Great Lakes: A History of Passenger Steamships on the Inland Seas. Ann Arbor: University of Michigan Press.

[2] https://commons.wikimedia.org/w/index.php?curid=42014

[3] Ian Roberts, 2017, Steam handbook: An introduction to steam generation and distribution. Endress, Hauser Flowtech AG, Press.

[4] https://insulation.org/io/articles/the-history-of-the-steam-generating-boiler-and-industry/

[5] SiO, 2006, DNV Auxiliary boiler survey & Machinery, DNV press.

[6] Board, ”The National board of boiler and pressure vessel inspector,” *bulletin*, vol. 58, nr 2, p. 19, 2003.

[7] "Fatigue under Thermal and Mechanical loading:Mechanisms,Mechanics and Modelling.," in *EUR 16353 EN*, pettern, Netherland, 1995.

[8] https://thewbia.com

[9] K B Mcintyre, 2002. A Review Of The Common Causes Of Boiler Failure In The Sugar Industry Alstom Power - John Thompson Boiler Division, Cape Town, South Africa.

[10] National Bureau of Standards, 1983. The Economic Effects of Fracture in the United States. Department of Commerce., U.S.

[11] J. J. T. S. Board, 2017. Marine Accident Investigation Report, JSTB MAR2017-12.

[12] Barsoum, Z., 2008. Residual Stress Analysis and Fatigue Assessment of Welded Steel Structures, KTH, School of Engineering Sciences, Stockholm, Sweden.

[13] D. N. Inge Lotsberg, 2016. Fatigue design of marine structures, New York NY: New York NY : Cambridge University Press, U.S.A

[14] Amiri, Michael M. Khonsari , 2013. Mehdi, Introduction to thermodynamics of Mechanical Fatigue, CRC Press, , pp. 1-164

[15] Lindström, P. R. M., 2015, Non-linear fracture mechanics in LS-DYNA and, i *10th European LS-DYNA Conference*, Würzburg, Germany, 2015

[16] ASTM Standards, 2013. Standard test for measuring of fracture toughness, ASTM E1820-13, American Society for Testing and Material ,Philadelphia, U.S.A.

[17] BSI Standards, 2015. Guide to methods for assessing the acceptability of flaws in metallic structures, London.

[18] Joacim Castenson & Moa Grandis , 2018. ” Fatigue analysis of marine boiler Sunrod CPDB12,” Linnaeus University, Växjö, Sweden.,

[19] A. F. Molland, 2008. The Maritime Engineering References book,: Elsiever ltd, U.S.A.

[20] H.C. Theisens (2016) Lean Six Sigma, 4th Edition, Lssa B.V. Amsterdam

[21] USA National Laboratories, https://nationallabs.org/site/wp-content/uploads/2017/05/National-Labs-all-r.pdf

[22] https://www.incose.org/

[23] https://www.incose.org/products-and-publications/se-handbook

[24] https://www.nasa.gov/seh/2-fundamentals

[25] https://www.nasa.gov/connect/ebooks/nasa-systems-engineering-handbook

[26] Newman, J.N. 1997. Marine Hydrodynamics. Cambridge, Massachusetts, the MIT Press, Washington, D.C.

[27] DNVGL 2017, Rules of Classification: DNVGL-RU-SHIP.

[28] Triantafyllou M.S. & Hover F.S. 2003. Manoeuvring and control of marine vehicles, Department of Ocean Engineering, Massachusetts Institute of Technology, Cambridge, Massachusetts USA.

[29] Lloyd, A.R.J.M, 1989. Seakeeping: Ship Behaviour in Rough Weather, Ellis, Horwood Ltd.

[30] Anderson, T. L., 2005, Fracture Mechanics--Fundamentals and Applications, 3rd Ed., CRC Press, Boca Raton, FL. U.S.

[31] Hobbacher, A., Recommendation for fatigue Design of Welded Joints and Components, The international Institute of Welding, IIW-1823-07 ex. XIII-2151r4-07/XV-1254r4-07, (2008).

[32] Rice J. R., A Path Independent Integral and the Approximate Analysis of Strain Concentration by Notches and Cracks, Journal of Applied Mechanics, 35, 1968, pp. 379-386.

[33] Lindström, P. R. M, 2015, Improved CWM platform for modelling welding procedures and its effects on structural behaviour, Dotoctoral thesis, University West, Trollhatan, sweden.

[34] William F. Hosford, 2017. Mechanical Behavior of Materials, Cambridge University Press, Assembly," i *International institute of welding*, Shangai, china,

[35] Bower, A .F, 2010, Applied Mechanics of Solids, ISBN 978-1-4398-0247-2 ,, CRC Press Taylor & Francis Group, Boca Raton,Florida U.S.A,, pp. 115-124

[36] Raju, I. S. and Newman, 1. c., Jr. (1982) Stress intensity factors for internal and external surface cracks in cylindrical vessels. ASME J. Pres. Yes. Tech. 104, 293-298.

[37] Niemi, E., 1995. Stress determination for Fatigue Analysis of Welded Components, IIW doc. IIS/IIW-1221-93, The Iternational Institute of Welding.

[38] LS-DYNA, 2018. Keyword User's manual, version 971 Volume 1, Livemore Software Technology Corporation (LSTC), Livermore CA . USA.

[39] Radaj, D., Sonsino, C. M., Fricke, W., 2006. Fatigue Assessment of Welded Joints by Local Approaches. 2. Ed, Woodhead Publishing, Cambridge, .

[40] Lotsberg, I., Sigurdsson, G., 2006. Hot Spot Stress S-N Curve for Fatigue Analysis of Plated Structures, Journal of Offshore Mechanics and Arctic Engineering, Vol.128)